



# The study of the high-density gas distribution in SFRs with the SRT: the test cases of L1641-S3 and CepA-East

C. Codella<sup>1</sup>, M.T. Beltrán<sup>2,3</sup>, D. Panella<sup>2</sup>, R. Cesaroni<sup>2</sup>, R. Nesti<sup>2</sup>, and F. Massi<sup>2</sup>

<sup>1</sup> INAF - Istituto di Radioastronomia, Sez. di Firenze, Largo E. Fermi 5, I-50125 Firenze

<sup>2</sup> INAF - Osservatorio Astrofisico di Arcetri, Largo E. Fermi 5, I-50125 Firenze,

<sup>3</sup> Universitat de Barcelona, Dept. Astronomia i Meteorologia, Av. Diagonal 647, E-08028 Barcelona

## Abstract.

The star forming process occurs in molecular cores associated with high density and low temperature conditions. In addition, as the young stellar object evolves, its mass loss process interacts with the surrounding medium affecting the structure and the physical conditions of the natal cloud, often creating complex clumpy scenarios. The SRT antenna will allow one to survey star forming regions by using high-density standard tracers and obtaining high angular resolution maps. We present the results obtained from the 22-43 GHz observations of the NH<sub>3</sub>, HC<sub>3</sub>N, and HC<sub>5</sub>N emission carried out with the Medicina and Noto radiotelescopes. The complex CepA-East and L1641-S3 star forming regions have been used as test cases. In the light of the preliminary results of these projects we will discuss the steps ahead possible by the future use of SRT.

## 1. High-density gas in intermediate-mass star forming regions

The first stages of the star forming process are characterised by mass ejection in the form of molecular outflow, which is closely coupled with infall motions (e.g. Bachiller 1996). Once the protostar is formed, outflows are the main means of removing the material left over from the collapse of the natal cloud. However, it is not completely clear which are the effects that the parent molecular cloud has in determining the structure, orientation, and collimation degree of the outflows. Is there any dependence of these characteristics on the mass of the driving Young Stellar Object (YSO)? Compared to

their low-mass counterparts, these more massive outflows tend to be more chaotic and have more complex structures, and the nice bipolar morphology observed in many low-mass stars is not found towards them (e.g. Stanke et al. 2000; Fuente et al. 2001). However, these statements could not be reflecting reality but observational restrictions. The fact that intermediate-mass YSOs tend to be located at distances greater than those of low-mass counterparts, makes it very difficult to identify the youngest (proto)stars and to study them and the outflows powered by them with sufficient linear spatial resolution. In addition, the superposition of multiple outflows in intermediate-mass Star Forming Regions (SFRs), and the more complex environment itself, usually with

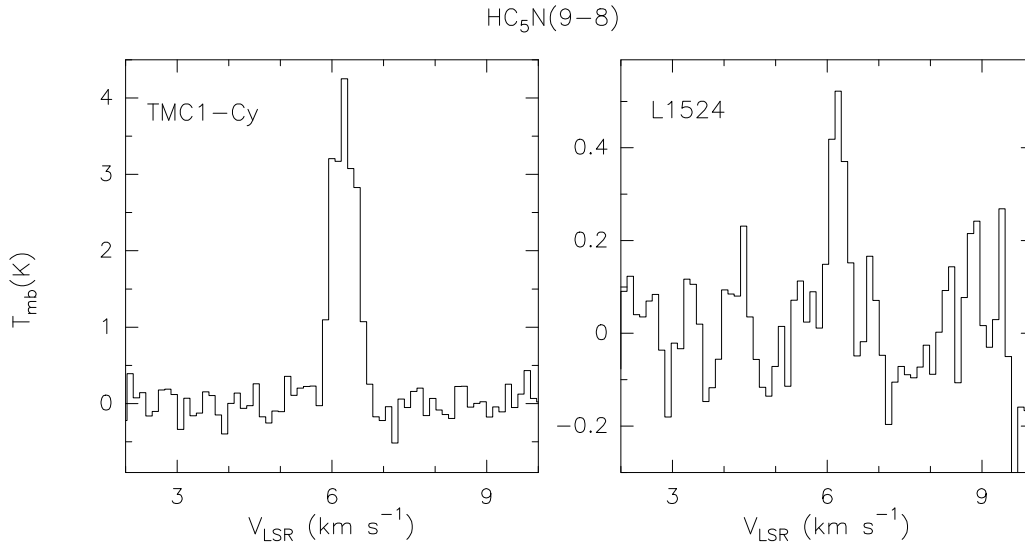


**Fig. 1.** Spectra of the  $\text{HC}_5\text{N}(9-8)$  line at 24.0 GHz observed towards the dark clouds TMC1-Cy and L1524. The observations have been performed during test runs with the 32-m Medicina antenna.

more than one embedded source and larger amounts of circumstellar material, can also contribute to the complex observed properties.

Two regions where to face these questions are L1641 and Cepheus A-East, which are clouds characterised by intermediate-mass SFRs and associated with numerous molecular outflows. We decided to study these regions by using tracers of high-density ( $\geq 10^4 \text{ cm}^{-3}$ ) molecular material. A classical choice is represented by  $\text{NH}_3$  and, in particular, by its (1,1) and (2,2) inversion transitions at 23.7 GHz. The frequency separation between the two lines is  $\sim 30$  MHz and thus both lines are usually observed with the same receiver configuration, with a consequent accurate measurement of the kinetic and excitation temperatures.

Also cyanopolyynes ( $\text{HC}_{2n+1}\text{N}$ ,  $n = 1, 2, 3, \dots$ ) can be used as tracers of high-density gas in SFRs. Several transitions due to different molecules lie in the frequency ranges allowed by the receivers mounted on the Medicina antenna. Since the  $\text{HC}_5\text{N}(9-8)$  line at 24.0 GHz had been easily detected towards dark clouds located in Taurus during test runs performed at Medicina during the last years (Fig. 1), we decided to search for this emission in L1641 and CepA-East. Unfortunately, we

detected no  $\text{HC}_5\text{N}(9-8)$  line towards these regions, and thus we decided to observe the  $\text{HC}_3\text{N}(5-4)$  emission at 45.5 GHz with the 32-m Noto radiotelescope.

In this paper, we present the preliminary results of the  $\text{NH}_3$  and  $\text{HC}_3\text{N}$  surveys of L1641 and CepA-East. We started the project by producing maps in order: (i) to prepare future observations with higher angular resolution, (ii) to understand the potential of these Italian antennas for observations and scientific goals like the present ones, and, in particular, (iii) to open, in the light of the SRT project, a discussion about the observational needs of the Italian star-formation groups.

## 2. Medicina and Noto observations and SRT perspectives

### 2.1. The $\text{NH}_3$ clumps and the L1641-S3 outflow

The first region of L1641 we mapped is L1641-S3, where Wilking et al. (1990) and Morgan et al. (1991) detected a CO outflow, whose geometry is not clear. Actually, while Wilking et al. (1990) found a definite overlap between the red- and blueshifted lobes suggesting a

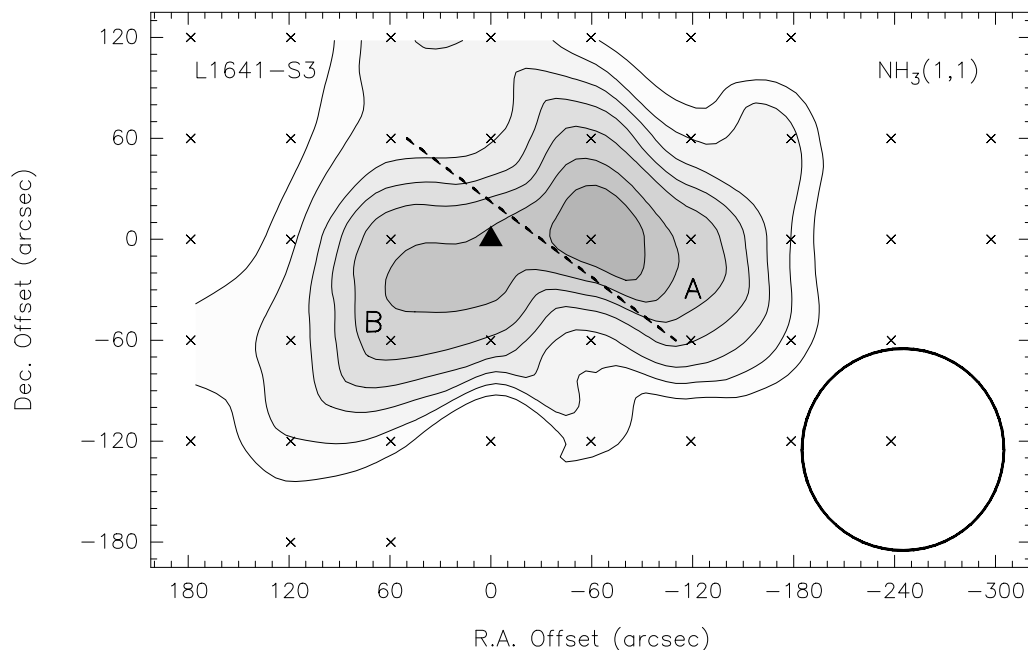


**Fig. 2.** Contour map of the  $\text{NH}_3(1,1)$  emission towards L1641-S3, calculated over the main line profile ( $1\text{--}9\text{ km s}^{-1}$ ) of the ammonia pattern (Beltrán et al. *in prep*). The empty circle shows the Medicina beam (HPBW), the small crosses mark the observed positions, while the filled triangle denotes the IRAS05375–0731 coordinates. The labels indicate the two  $\text{NH}_3$  clumps while the thick dashed line roughly indicates the direction of the main CO outflow axis according to Morgan et al. (1991).

flow lying along the line of sight, Morgan et al. (1991) found a bipolar distribution located along a direction close to the plane of the sky, pointed out by the thick dotted line in Fig. 2. NIR observations (Chen & Tokunaga 1994; Hodapp 1994) revealed a number of faint sources close to the position of IRAS05375–09731, which has a bolometric luminosity of  $\sim 80\text{--}90 L_{\odot}$ . The reddest NIR source, labeled L1641-S3, is thought to be the counterpart of the IRAS source (marked by a filled triangle in Fig. 2) and it is the candidate source driving the molecular outflow. Wouterloot et al. (1988) also detected  $\text{NH}_3$  emission indicating high-density conditions for the gas associated with L1641-S3, but the structure of the ammonia cloud has not been defined.

We mapped L1641-S3 in the  $\text{NH}_3(1,1)$  and (2,2) lines with the Medicina antenna. The maps have been produced by fully sampling the region with a spacing of  $60''$  ( $\sim \text{HPBW}/2$ ).

Figure 2 reports the  $\text{NH}_3(1,1)$  distribution: two clumps have been detected, the western and brightest one called A, and the eastern one called B. The ammonia emission shows an elongated flattened structure, roughly perpendicular to the CO molecular outflow as derived by Morgan et al. (1991), with the clumps A and B located at both sides of the molecular lobes. These results support the outflow geometry given by Morgan et al. (1991) and suggest that the two clumps could be tracing gas entrained within the surface of interaction between the molecular outflow and the dense ambient material, resembling what is found for another outflow driven by an intermediate YSO, IC1396N, by Codella et al. (2001) and Beltrán et al. (2002).

Selected positions of the  $\text{NH}_3$  map have been observed using the  $\text{HC}_3\text{N}(5\text{--}4)$  emission and the Noto radiotelescope. Figure 3 compares the  $\text{HC}_3\text{N}$  profiles with those of the

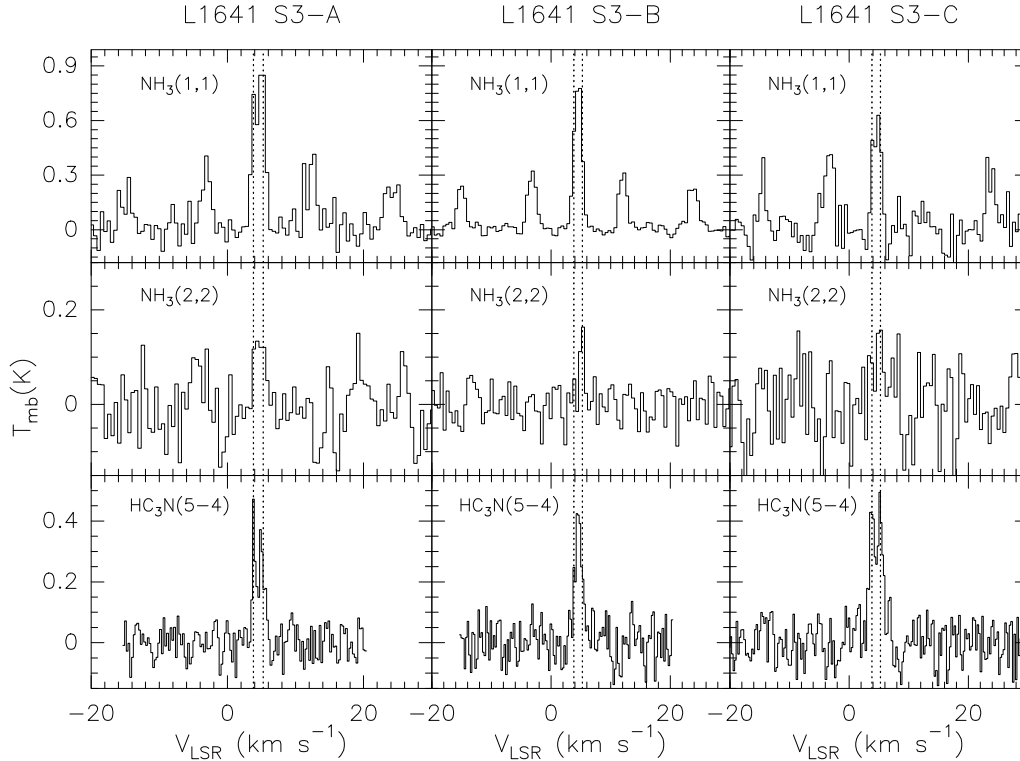


**Fig. 3.** Spectra of  $\text{NH}_3(1,1)$ ,  $\text{NH}_3(2,2)$ , and  $\text{HC}_3\text{N}(5-4)$  taken towards the positions of the ammonia clumps A (left panel), B (middle; see Fig. 2). The right panels report the spectra observed towards the  $(0'', +60'')$  map position (called C), where bright  $\text{HC}_3\text{N}(5-4)$  emission has been detected (Beltrán et al. *in prep*). Note that the  $\text{HC}_3\text{N}(5-4)$  spectra at positions A and C clearly show two spectral components, which are not clearly visible in the ammonia lines where different hyperfine components are blended. The two components (dotted lines) peak at  $+3.9$  and  $+5.0$   $\text{km s}^{-1}$ , respectively. The  $\text{HC}_3\text{N}(5-4)$  spectrum of clump B does not show a double-peaked structure, although the  $\text{NH}_3(2,2)$  profile suggests a weak emission at  $+5.0$   $\text{km s}^{-1}$ . The observations have been performed with the Medicina ( $\text{NH}_3$ ) and Noto ( $\text{HC}_3\text{N}$ ) radiotelescopes.

$\text{NH}_3(1,1)$  and  $(2,2)$  lines. The spectra refer to the positions of clumps A and B as well as to the  $(0'', +60'')$  map position (called C), where the preliminary  $\text{HC}_3\text{N}$  map (not shown here) suggests the occurrence of a bright emission peak. The  $\text{HC}_3\text{N}$  spectra clearly show two spectral components, which are not clearly visible in the ammonia lines where different hyperfine components are blended. The first component peaks at a velocity of  $+3.9$   $\text{km s}^{-1}$ , while the second one peaks at  $+5.0$   $\text{km s}^{-1}$ . The FWHM of these lines are in the  $1.0$ - $1.5$   $\text{km s}^{-1}$  range. Although one cannot exclude a sampling/resolution effect, the preliminary spectra reported in Fig. 3 seem to indi-

cate an  $\text{HC}_3\text{N}/\text{NH}_3$  emission ratio which depends on the map position. In order to confirm this scenario further analysis and observations able to reach angular resolutions around  $10''$ - $20''$  are required.

## 2.2. $\text{HC}_3\text{N}$ emission along the CepA-East southern outflow

Which is the potential of a high-density gas tracer such as  $\text{HC}_3\text{N}$  to clarify the pictures of complex SFRs associated with multiple outflows? We have used the Noto antenna and the CepA-East region trying to answer this ques-

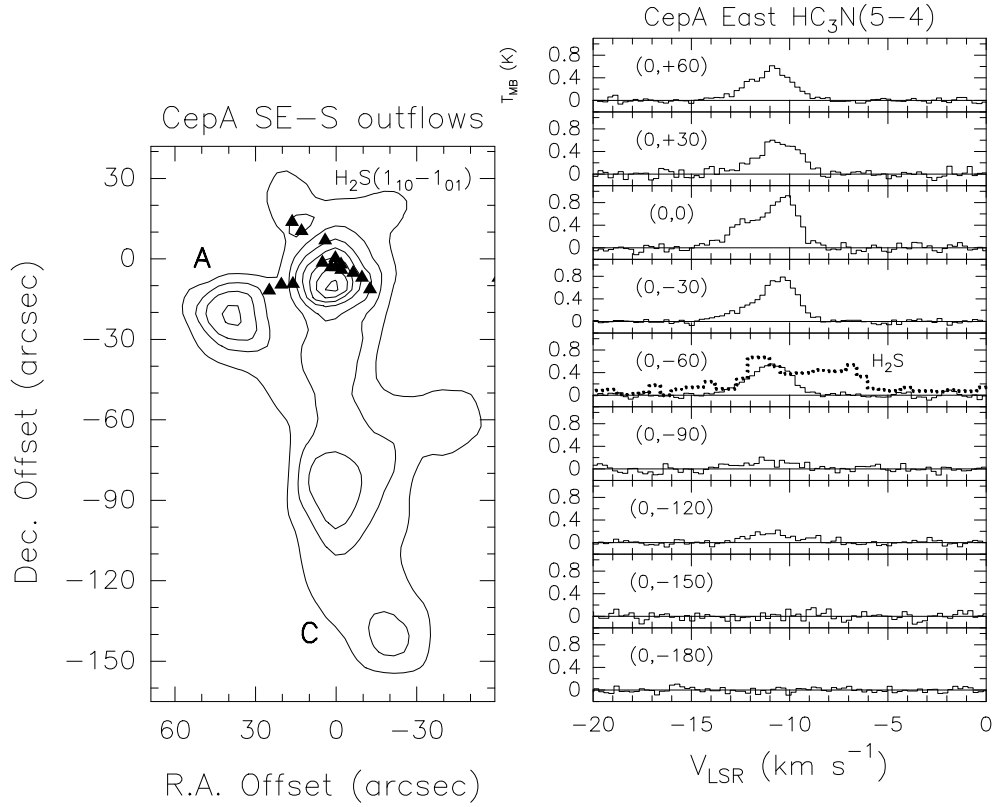


**Fig. 4.** Left: Contour maps of the  $\text{H}_2\text{S}(1_{10}-1_{01})$  redshifted emission (Codella et al. 2005) integrated over the velocity interval  $-7, -3 \text{ km s}^{-1}$ . Two main flows are clearly drawn: one pointing to SE (and ending at the clump A position), and another towards South (ending at clump C). The triangles mark the VLA 2 cm continuum knots which trace B-type stars driving three shocked strings. Right:  $\text{HC}_3\text{N}(5-4)$  line (45.5 GHz) profiles observed towards the main axis of the southern outflow with the 32-m Noto radiotelescope. Angular offset is indicated. Note that in the middle ( $0'', -60''$ ) panel the  $\text{HC}_3\text{N}$  profile is compared with the  $\text{H}_2\text{S}(1_{10}-1_{01})$  spectrum (divided by 1.8; dotted line) taken at the same position with the 30-m IRAM antenna.

tion. CepA-East is an intermediate-mass SFR harbouring an OB3 stellar association (Goetz et al. 1998, and references therein) driving a number of molecular outflows (see also the contribution by Codella et al. on protostellar outflows in the present Proceedings). In summary, there is a central outflow lying in the NE-SW direction, an eastern outflow pointing towards SE, and, in addition, a quite extended (0.6 pc) redshifted outflow which is moving towards South. The latter outflow has been discovered only thanks to  $\text{H}_2\text{S}$ ,  $\text{SO}_2$ , and  $\text{HDO}$  emissions (Codella et al. 2003, 2005), and thus

results to be associated with conditions particularly favourable to a chemical enrichment of the gas surrounding the YSO due to the passage of shocks. Fig. 4 (left panel) shows the contour map of the  $\text{H}_2\text{S}(1_{10}-1_{01})$  emission, observed at 168.8 GHz with the 30-m IRAM antenna, integrated over the redshifted interval typical of the southern outflow. The triangles stand for the Very Large Array (VLA) cm-continuum components which trace the YSOs driving outflows and shocks associated with the central and eastern outflows. From Fig. 4 it is possible to detect the redshifted component

of the SE outflow (ending at the position of the clump called A) and the southern outflow, which extends at the position of the clump C).

As a first step of the project, the CepA-East southern outflow has been observed using the HC<sub>3</sub>N(5–4) line, with the Noto antenna and fully sampled with a spacing of 30'' (~HPBW/2): the resulting spectra are reported in the right panel of Fig. 4. Different positions are associated with different line profiles. The (0,0) position, centered on the YSO association, shows a spectrum with a main peak at  $-10 \text{ km s}^{-1}$ , which is the LSR velocity of CepA-East, and, in addition, a blueshifted secondary peak around  $-13 \text{ km s}^{-1}$ , probably tracing outflow motions. In particular, since a blueshifted emission is clearly observable in all the spectra between the (0'',+60'') and (0'',-60'') positions, this could trace the blueshifted lobes of the eastern and central outflows. This conclusion is supported by a shift of the main peak towards bluer velocities in the (0'',+60'') and (0'',-60'') spectra, which do not sample the central region hosting the YSOs. On the other hand, there is no clear indication of a bright redshifted emission in the HC<sub>3</sub>N spectra, suggesting a relatively low-density condition ( $\leq 10^4 \text{ cm}^{-3}$ ) for the southern outflow. In the (0,-60'') panel, the HC<sub>3</sub>N(5–4) spectrum is compared with the H<sub>2</sub>S(1<sub>10</sub>-1<sub>01</sub>) profile, taken with the 30-m IRAM antenna: it is possible to see that the H<sub>2</sub>S/HC<sub>3</sub>N ratio is strongly dependent on the velocity, and that the redshifted H<sub>2</sub>S regime has no HC<sub>3</sub>N counterpart. These results call for further HC<sub>3</sub>N observations with higher angular resolution in order to disentangle and to map different gas components such as high-density clumps and outflow lobes minimising effects due to beam dilution.

From Fig. 4, it is easy to see the advantages given by a HPBW smaller than the 60'' of the Noto radiotelescope. In particular, it would be extremely important to reach angular resolutions matching those typical of a mm-antenna like the 30-m IRAM telescope: e.g. the H<sub>2</sub>S emission reported in Fig. 4 has been observed with a HPBW  $\approx 14''$ .

*Acknowledgements.* We are grateful to C. Buemi, G. Comoretto, P. Leto, F. Palagi, C. Trigilio, and G. Umana for their help during the Noto and Medicina observations.

## References

- Bachiller, R. 1996, ARA&A, 34, 111  
 Beltrán, M.T., Girart, J.M., Estalella, R., Ho, P.T.P., & Palau, A. 2002, ApJ, 573, 246  
 Chen, H., & Tokunaga, A.T. 1994, ApJS, 90, 149  
 Codella, C., Bachiller, R., Nisini, B., Saraceno, P., & Testi, L. 2001, A&A, 376, 271  
 Codella, C., Bachiller, R., Benedettini, M., & Caselli, P. 2003, MNRAS, 341, 707  
 Codella, C., Bachiller, R., Benedettini, M., et al. 2005, MNRAS, 361, 244  
 Fuente, A., Neri, R., Martín-Pintado, J., et al. 2001, A&A, 375, 1018  
 Goetz, J.A., Pipher, J.L., Forrest, W.J., et al. 1998, ApJ, 504, 359  
 Hodapp K.-W. 1994, ApJS, 94, 615  
 Morgan, J.A., Schloerb, F.P., Snell, R.L., & Bally, J. 1991, ApJ, 376, 618  
 Stanke, Th., McCaughrean, M.J., & Zinnecker, H. 2000, A&A, 355, 639  
 Wilking, B.A., Blackwell, J.H., & Mundy, L.G. 1990, AJ, 100, 758  
 Wouterloot, J.G.A., Walmsley, C.M., & Henkel, C. 1988, A&A, 203, 367